Heuristics for revealing the event structure of neuronal spike trains

J. Vincent Toups[1], Jean-Marc Fellous[2], Terrence J. Sejnowski[3,4] and Paul Tiesinga[1],

[1]Computational Neurophysics Laboratory, Department of Physics & Astronomy, University of North Carolina, Chapel Hill, United States.
[2]Psychology Department and Program in Applied Mathematics, University of Arizona, Tucson, United States
[3]Computational Neurobiology Lab and Howard Hughes Medical Institute, Salk Institute, La Jolla, United States
[4]Division of Biological Sciences, University of California at San Diego, La Jolla, United States

568.7 KK16

Introduction

Neurons in sensory systems are likely to convey information about the temporal structure of stimuli. In vitro, single neurons respond precisely and reliably to the repeated somatic injection of the same fluctuating current on multiple trials, producing regions of elevated firing rate, which are termed events. Further analysis reveals spike patterns, which are trial-to-trial correlations between spike times (Fellous et al, J. Neurosci 2004). Finding events in data with realistic spiking statistics is challenging because events may overlap. Overlapping events typically belong to different spike patterns. Therefore, we developed a method to find spiking events that uses information about which pattern a trial belongs to. The procedure can be applied to spike trains of the same neuron across multiple trials to detect and separate responses obtained during different brain states. The procedure can also be applied to spike trains of multiple neurons, representing network activity, in order to extract volleys of near synchronous activity or to distinguish between excitatory and inhibitory neurons.

1

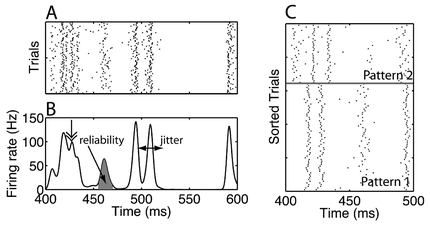

Figure 1. *Spike trains can be characterized in terms of events.* (A) A rastergram with spike trains obtained from a model neuron in response to the same fluctuating current waveform presented multiple times. There are vertical bands corresponding to spike alignments, each of which is an event. (B) The spike time histogram, with peaks corresponding to spike alignments (events). When peaks are isolated it is easy to assign each spike to an event. However, the assignment is made difficult by the presence of overlapping peaks (double arrow). (C) When the trials are sorted using the clustering algorithm, spike patterns emerge. The horizontal line separates two spike patterns.

2

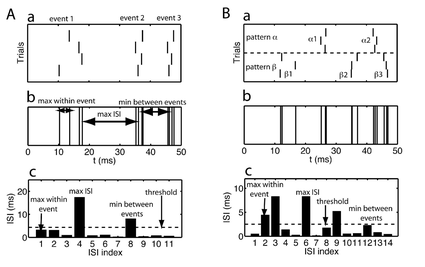

Figure 2. *It is not always possible to choose an appropriate threshold for the interval method.* (A-B) In each panel, we show, from top to bottom, (a) the rastergram, (b) the aggregate spike train and (c) the ISI time series. The relevant time scales are indicated in the graph. An estimate for the threshold, 0.1 times the maximum ISI, is shown as a dashed line in panel c. (A) An example with one spike pattern where an appropriate threshold can be chosen that is higher than the maximum ISI within an event but less than the minimum ISI between events. (B) An example with two spike patterns where there is no such threshold that separates within-event intervals from those between events.

References

Bair W, Koch C (1996) Neural Comput 8:1185-1202.
Bezdek JC (1981) Pattern recognition with fuzzy objective function algorithms. New York: Plenum. Buia C, Tiesinga P (2006) Journal of Computational Neuroscience 20:247-264.
Buracas GT, Zador AM, DeWeese MR, Albright TD (1998) Neuron 20:959-969.
de la Rocha J, Doiron B, Shea-Brown E, Josic K, Reyes A (2007) Nature 448:802-806.
Duda RO, Hart PE, Stork DG (2001) Pattern classification, 2nd Edition: Wiley.
Ermentrout GB, Galan RF, Urban NN (2008) Trends Neurosci.
Fellous JM, Tiesinga PH, Thomas PJ, Sejnowski TJ (2004) J Neurosci 24:2989-3001.
Fellous JM, Houweling AR, Modi RH, Rao RP, Tiesinga PH, Sejnowski TJ (2001) J Neurophysiol 85:1782-1787.
Jolliffe IT (2002) Principal component analysis, 2nd Edition. New York: Springer.
Mainen ZF, Sejnowski TJ (1995) Science 268:1503-1506.
Markowitz DA, Collman F, Brody CD, Hopfield JJ, Tank DW (2008) Proc Natl Acad Sci U S A 105:8422-8427.
Mishra J, Fellous JM, Sejnowski TJ (2006) Neural Netw 19:1329-1346.
Pal NR, Bezdek JC (1995) Ieee Transactions on Fuzzy Systems 3:370-379.
Rieke F, Warland D, de Ruyter van Steveninck RR, Bialek W (1997) Spikes: exploring the neural code. Cambridge: MIT press.
Salinas E, Sejnowski TJ (2001) Nature Reviews Neuroscience 2:539-550.
Tibshirani R, Walther G, Hastie T (2001) Journal of the Royal Statistical Society Series B-Statistical Methodology 63:411-423.
Tiesinga P, Fellous JM, Sejnowski TJ (2008) Nat Rev Neurosci.
Tiesinga PH, Fellous JM, Sejnowski TJ (2002) Neural Comput 14:1629-1650.
Tiesinga PHE, Toups JV (2005) Journal of Computational Neuroscience 18:275-286.
Victor JD, Purpura KP (1996) J Neurophysiol 76:1310-1326.
Womelsdorf T, Schoffelen JM, Oostenveld R, Singer W, Desimone R, Engel AK, Fries P (2007) Science 316:1609-1612.

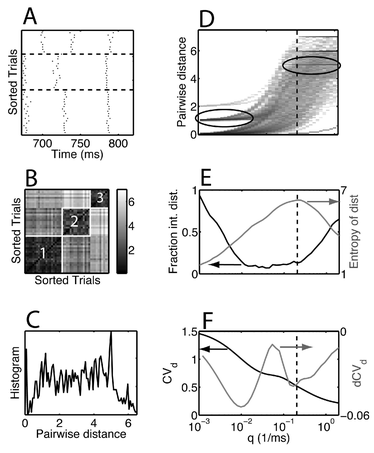

3

Figure 3. *The temporal resolution parameter q was determined using a heuristic on the distance distribution.* (A) Rastergram of 45 trials containing three patterns. (B) The distance matrix for the below-determined q value. The matrix has a diagonal structure with blocks of small distance values corresponding to the patterns (as labeled by numbers inside the blocks). (C) The histogram of the matrix elements of the distance matrix shown in panel B. (D) Density plot of the distance distribution as a function of q. The ellipses highlight examples of enhanced density for integer values for the distance for small and large values of q. Panels D-F have a common x-axis scale, which is shown in panel F. (E) We show (black curve, left-hand-side scale) the fraction of distances within 0.05 from an integer and (gray curve, right-hand-side scale) the entropy of the distance histogram as a function of q. (F) We show (black curve, left-hand-side scale) CV of the distances and (gray curve, right-hand-side scale) the differenced CV. The q value chosen by the heuristic is the mean of the q-value at which the entropy has a maximum and the location of the deepest trough in the dCV_d that occurs after the highest peak.

4

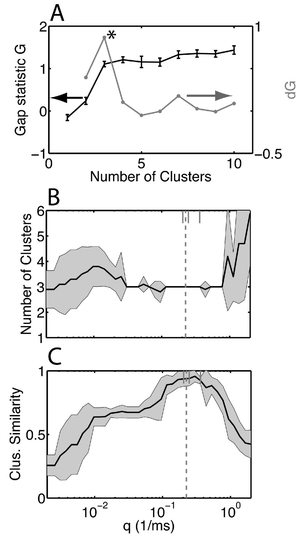

Figure 4. *The heuristics for finding the q value and the number of clusters perform well for artificial data sets.* (A) We show (black curve, left-hand-side scale) the gap-statistic G and (gray curve, right-hand-side scale) its difference dG as a function of the number of clusters. The number of clusters N_c reached after the highest increase in the gap-statistic (at the peak of dG indicated by the asterisk) is selected as a heuristic for the number of clusters in the data. (B) We generated ten independent artificial data sets of 45 trials with three patterns all with the same statistics as those shown in Figure 3. The average N_c value picked by the heuristic is plotted as a function of q, the shaded area represents the standard deviation. (C) The similarity between the clustering obtained with the selected N_c value and the known classification as a function of q. The black line is the mean and the shaded area represents the standard deviation. The dashed line in B and C is the mean value of the q value picked by the heuristic, the choice for each of the ten data sets is indicated by the ticks at the top of the graph. The heuristically picked q value leads to an optimal similarity and an N_c that is equal to the actual number of clusters present in the data.

5

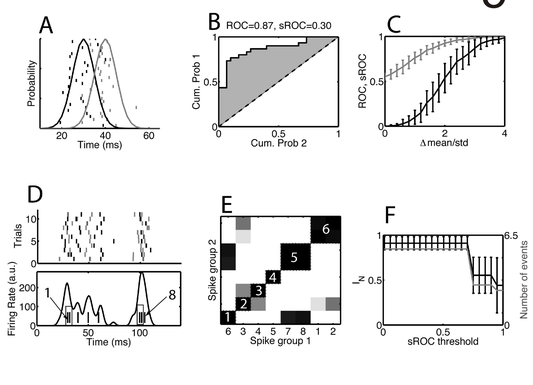

Figure 5. *The ROC-based criterion for merging events common across multiple patterns.* (A) Thirty trials of (black ticks) spikes drawn from a (black curve) Gaussian with a mean of 30 ms and thirty trials of (gray ticks) spikes drawn from a (gray curve) Gaussian with mean 40 ms. (B) The ROC curve was estimated as the cumulative distribution of the first group of spikes plotted versus that of the second group of spikes. The scaled ROC (sROC) was obtained by dividing the ROC area above the diagonal by 0.5 and taking the fourth power. (C) The same procedure was repeated for different values of the difference in means between the two distributions. We show the (gray curve) ROC and (black curve) sROC area versus the difference of theoretical means over the standard deviation. (D) Eleven trials of an example data set consisting of 8 events. In (top) the rastergram the events are sorted by their theoretical means, with the corresponding spikes rendered alternately in gray and black. (Bottom) the histogram obtained from one realization of the data set. The ticks at the bottom represent the theoretical means of the events and are labeled 1 to 8, with the events to be merged shown in a box. (E) Matrix of sROC distances between the events. The events are ordered (the numbers on the x-axis correspond to those in panel D) according to a hierarchical clustering with an sROC threshold of 0.5. (F, black curves) The normalized mutual information between the classification using clustering and the desired cluster and (gray curves) the number of events remaining after merging. The error bars on the mutual information represent the standard deviation across 100 independent realizations of the data set.

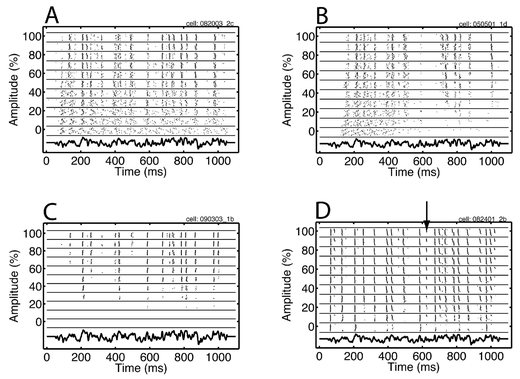

7

Figure 7. *The procedure for detecting and characterizing events.* (A) Rastergram of the data in Figure 6A for an amplitude of 70% and the time segment between 650 ms and 850 ms. (B) Distance matrix for the trials shown in panel A. The range from small to large distances is mapped onto a gray scale going from dark to white. (C) The heuristic for determining q is based on the distribution of the elements of the distance matrix, referred to as the distances. We show (black curve, left-hand-side scale) the dCV_d and (gray curve, right-hand-side scale) the entropy of the distances as a function of q. The q value chosen by the heuristic is the mean of the q-value at which the entropy has a maximum and the location of the deepest trough in the dCV_d that occurs after the highest peak. (D) The heuristic for determining the number of spike patterns. We show the (black curve, left-hand-side scale) $G(N_c)$ and (gray curve, right-hand-side scale) $dG(N_c)$. The errorbars are the standard deviation obtained across 50 surrogates. The value of N_c chosen by the heuristic is the one for which the dG is maximal (asterisk). (E) Rastergram and (F) distance matrices with the trials reordered according to their cluster membership. The horizontal lines in (E) separate the clusters and the vertical gray bands are the events. On two instances events common to more than one cluster were merged as indicated by the arrows.

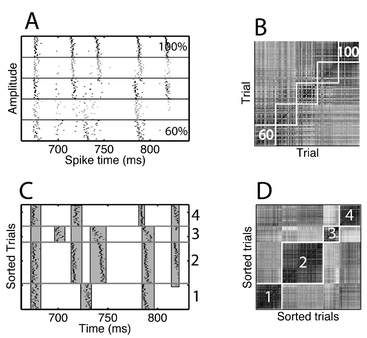

6

Figure 6. *Rastergrams obtained in response to injection of the same fluctuating current waveform for four different layer 5 prefrontal cortical neurons, recorded in vitro.* Each line in the rastergram represents a spike train obtained on a trial, with the x ordinate of each tick being the spike time. The spike trains are ordered in blocks (delineated by horizontal lines) based on the amplitude of the injected current, expressed as a percentage, with the highest amplitude on top. Within each block the trials are ordered as they were recorded, with the earliest trial at the bottom. The injected current is shown for one amplitude at the bottom. Each panel shows the response of an example cell.

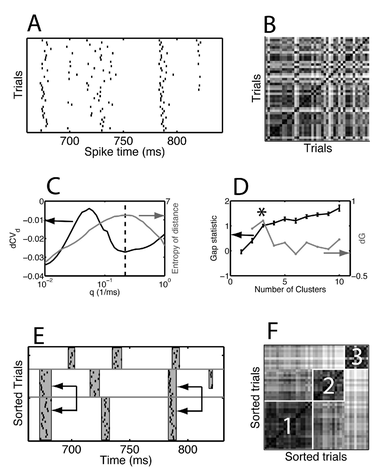

8

Figure 8. *Spike patterns persisted across multiple amplitudes.* (A) The rastergram for the data shown in Figure 6A for amplitudes between 60% and 100% and during the time segment between 650 ms and 850 ms. (B) The corresponding distance matrix obtained for the q values selected by the heuristic. (C, D) The gap-statistic suggested that there were four patterns. We show the (C) rastergram and (D) distance matrix with the trials sorted according to their cluster membership. The numbers are the cluster index. The gray vertical bands show the detected events that remained after applying the merging procedure.

Conclusion

We developed a four-step procedure with a few parameters to determine the event structure of a set of spike trains: (1) Determine the appropriate q-value (Panel 3); (2) Determine the number of patterns N_c (Panel 4); (3) Find the events using the interval method applied to each pattern separately (Panel 2); (4) Merge events common among spike patterns (Panel 5).

This procedure is broadly applicable. The histogram needs to be peaked, which is indicative of events, and if there are overlapping peaks, they should be due to multiple spike patterns. The procedure was tested using artificial data with spike patterns. It was also applied to spike trains recorded in response to the same fluctuating current injected across multiple trials (Panels 6 to 8). The method uncovered evidence for spike patterns in these data. The procedure can also be applied to groups of neurons, for instance a set of inhibitory and excitatory neurons. It can then be used to separate the inhibitory and excitatory responses and determine the precision and relative lag, which is the subject of experimental and theoretical studies (Buia and Tiesinga, 2006; Mishra et al., 2006; Womelsdorf et al., 2007).

This work was supported by NIH grant MH68481.